Improving the Landcover Classification using Domain Knowledge

Christine Largouët[1] and **Marie-Odile Cordier**[2]

Abstract. This paper [3] deals with the integration of domain knowledge to improve the landcover classification of a sequence of images. This new approach consists in representing the plot of land as a dynamic system and in modeling its evolution (knowledge about crop cycles, rotations and farmer practices) with the timed automata formalism. The main feature of this work is to improve the classification provided by a traditional classification with data resulting from the simulation of the plot evolution model. The aim of this paper is to focus on the experiments carried out on a sequence of five images. The problem of classification refinement and the model used to capture domain knowledge are first presented. The emphasis is then put on the results and their interpretation that show the contribution of the method to improve the classification of images.

Keywords. Dynamic Plot Modeling, Landcover Classification, Image Interpretation, Model-Based Reasoning, Temporal Reasoning.

1 INTRODUCTION

The analysis of landcover and the monitoring of environmental changes of an agricultural area is one of the major application of remotely-sensed images. For the last two decades, numerous work have been proposed regarding the landcover classification and most of the methods are based on the spectral analysis of individual pixels. If the main interest of these techniques is to automatically classify the images, the results they provide cannot rival with those obtained by human photo-interpreters. However, with the increasing use of digital geographic information and since the thematic map is an important layer in geographic information systems (GIS), the quality of the classification has received renewed interest. Misclassification resulting from usual classifiers is distinguished into two aspects [5]: misclassification in the strict sense and mislabeling. Misclassification is due to spectral confusion between landcover types whereas mislabeling occurs when information about the classes is insufficient to determine, for some particular pixels, to which class they belong. To improve the classification accuracy of traditional classifiers, several statistical models, using or not ancillary data, have been proposed. Within the Artificial Intelligence field, knowledge-based systems incorporate image context and spectral characteristics in a rule-based classification [12, 7, 9]. Spatial information such as proximity, connection, relative orientation and properties like size, and shapes of objects are used to help the identification of objects [13, 15, 8]. The idea retained from these approaches is that the area of study is viewed as the composition of small homogeneous segments and the classification process involves a spectral classification and a rule-based classification of the segments. These methods are usually used to landuse classification [8] or to scene interpretation, such as the recognition of airport [13], but they are not sufficient to classify landcover since the spectral classification is used as a basis and is not discussed afterwards. In order to minimize the ambiguity between the classes, systems have proposed to use multi-source information like images from different sensors [4] or data extracted from GIS [6, 1]. If these systems provide discrimination between the classes for several ambiguous pixels, they require a large amount of information which is not always available. According to some authors [14, 11], we suggest to use the conjunction of multi-seasonal remotely-sensed images to discriminate between different categories of vegetation. This new approach differs from the ones mentioned above in that it relies on the classification of plots of land and not of pixels.

The aim of this paper is to present this new approach used to improve the landcover classification. We propose to work on a sequence of images and to use the dynamics of the object we want to classify, i.e. the plot of land. The idea consists in modeling the evolution of the plot and comparing the expected state obtained by a model simulation, in order to improve the classification of images. To model the evolution of a plot, we have chosen a modeling independent of the sensors that can be easily built from expert knowledge. A preliminary per-plot classification is applied on images which provides a set of all plausible classes for each plot. Knowledge about crops such as main crop states, crop cycle evolution and rotation practices are described in the timed automata formalism [2]. The method, used to refine the classification, relies on prediction and postdiction mechanisms where the model is used to give the expected state of the plot at each date referred to here as time. The method and the refinement algorithm are described in detail in [10]. In this paper, we focus on the experiments and on the interpretation of the results. This approach has been applied on the images of an environmental project called “Bretagne Eau Pure” in which the landcover map is a fundamental feature regarding water pollution. A sequence of five images (aerial, SPOT, LANDSAT) of a watershed near Rennes (France) is available. They were taken at different dates, in winter, spring and summer, and each image contains about 2000 plots of land, we aim to classify into seven or eight classes known *a priori*.

The remainder of this paper is organized as follows. Section 2 presents the data set used for the study and the preliminary classi-

[1] ENSAR, 65 rue St Brieuc 35042 Rennes cedex & IRISA, campus de Beaulieu 35042 Rennes cedex, France, email: clargoue@irisa.fr

[2] USARQ-INRA, 65 rue St Brieuc 35042 Rennes cedex & IRISA, campus de Beaulieu 35042 Rennes cedex, France, email: cordier@irisa.fr

[3] This paper has been accepted at the XIX^{th} Congress of the International Society for Photogrammetry and Remote Sensing (ISPRS 2000).

image	date	source	resolution	bands	number of landcover types
1	18/04/1997	aerial	2.5 m	1 (blue), 2 (green), 3 (red)	7
2	28/07/1997	LANDSAT TM	30 m	1 (0.45-0.520μm), 2 (0.53-0.61μm), 3 (0.62-0.69μm) 4 (0.78-0.91μm), 5 (1.55-1.75μm), 7 (2.08-2.35μm) 6 (10.4-12.5μm)	7
3	05/12/1997	SPOT	20 m	1(0.5-0.59μm), 2(0.61-0.68μm), 3(0.79-0.89μm)	7
4	25/05/1998	SPOT	20 m	idem	7
5	07/08/1998	SPOT	20 m	idem	8

Table 1. Characteristics of the initial images

fication. Section 3 defines the refinement problem and the prediction and postdiction mechanisms used to improve the classification of a sequence of images. Section 4 presents the timed automata formalism and the plot evolution model. In section 5 we discuss experimental results obtained by this new approach. We conclude and describe directions for future research in Section 6.

2 Preliminary classification

The area of study is a watershed located near Rennes in Brittany (France). Brittany is concerned about the water quality because of undesirable effects of pesticide and nitrate from fertilizers used to assure optimum plant growing. These substances leach into the rivers and contaminate well water. In order to best manage practices and minimize the risk of pollution, the first step of the project “Bretagne Eau Pure” is to precisely know the landcover of the studied watershed.
The data sources available are five aerial and satellite images covering nearly two agricultural cycles. Each image contains 2124 plots. Thanks to human observation, a ground truth is available on about 5% of the plots for each image. The ground truth allows us to know *a priori* the number of classes for each image. The characteristics of the images are shown in Table 1.

The landcover types known *a priori* are the following.
Image1: wheat, grassland, bare soil, barley, forest, water, urban.
Image2: wheat, grassland, corn, water, forest, stubble, urban.
Image3: wheat, grassland, other, bare soil, forest, water, urban.
Image4: wheat, grassland, corn, other, forest, water, urban.
Image5: wheat, grassland, corn, other, forest, water, urban, stubble.

The per-plot classification has been implemented using the Arkemie classification software [3]. The objective of this preliminary classification is to be an automatic process as simple as possible in the parameter choices. Arkemie computes for each region and each band, attributes such as average value, standard deviation, third order and fourth order moments. For the aerial and the SPOT images, the attributes used for the classification are the average value and the standard deviation on each band (1,2,3). For the LANDSAT TM image, the attributes used are the average value and the standard deviation on the bands 1,2,3,4,5 and 7, chosen for their complementarity.

Since a ground truth is available, we have preferred a supervised classification to an unsupervised one. The method used is the normal densities based quadratic classification which is almost identical to the linear classifier based on normal densities, but calculates covariance matrices for each individual class. The result of the classification is, for each plot, a probabilistic distribution over the classes. Two thresholds are used to select the more significant classes. Classes proposed with a probability under a *minimum threshold* are discarded from the plausible classes and conversely if a class has a probability over a *maximum threshold* it is considered as the class of the plot. Once the threshold process has been applied, the distribution of probabilities is renormalized for each plot. Several values have been tested for this two thresholds. A value under 0.9 for the maximum threshold attaches two much importance to the results given by the preliminary classification, since more than a half of the number of plots are already identified after this first classification. The maximum threshold is then fixed to 0.9 and for the minimum threshold, the value of 0.1 has been chosen as a good compromise.

In order to assess the accuracy of an image classification, we have defined two criteria. The first one represents the ambiguity rate on each image, the second one is sample-based and detects the misclassification in the strict sense. Three qualitative types on plots allow us to represent the ambiguity rate.

- *Clear* plot: the plot is identified by only one class.
- *Ambiguous* plot: the plot is identified by several classes.
- *Non-labeled* plot: the plot is not identified (Arkemie has encountered difficulties in labeling too small plots).

The sample-based method relies on the creation, for each image, of an error matrix which is the standard convention to represent the classification accuracy [5]. In an error matrix, the reference data (samples) are usually represented by the columns and the classified data are represented by the rows. The identification rate (or overall rate [5]) is calculated by dividing the total correct (i.e., the sum of the entries that form the major diagonal) by the total number of sample plots. The identification rate for the Image I_i is called τ_i. To create the error matrix, the class chosen as labeling the plot is the one having the maximum of probability.
Table 2 describes the results provided by the preliminary classification. The results show, for each image I_i, the identification rate τ_i, the number and the percentage of clear plots, ambiguous plots and non labeled plots.

I_i	τ_i	clear plots		ambiguous plots		non-labeled plots	
I_1	90.91%	1788	84.2%	330	15.5%	6	0.3%
I_2	89.29%	1697	79.9%	386	18.2%	41	1.9%
I_3	75.68%	796	37.5%	1306	61.5%	22	1%
I_4	64.49%	958	45.1%	1161	54.7%	5	0.2%
I_5	63.55%	541	25.5%	1583	74.5%	0	0%

Table 2. Preliminary classification results

3 Refinement problem

This section presents the general refinement problem as the landcover classification of a sequence of images $I_1, \cdots, I_n$ taken at time $t_1, \cdots, t_n$. Images may have been acquired by different sensors as they represent the same landscape area. The result of the preliminary classification is a collection of observations, each one referring to an agricultural plot of the area. The problem is to improve the classification we get for a plot on the n images and this will be referred to as refinement of the classification. We give the sketch of the corresponding algorithm.

for each image I_i
  for each plot P
    preliminary classification $\longrightarrow O_i$
for each plot P
  refinement of the classification
    $(\mathcal{A}, [O_1, \cdots, O_n]) \longrightarrow [K_1, \cdots, K_n]$

Let $\mathcal{C}$ be the set of classes. We denote O_i the observation about a plot P at time t_i. $O_i \subseteq \mathcal{C}$ is the set of all plausible classes describing the plot and resulting from the classification of the image I_i. The refinement problem takes as input the pair $(\mathcal{A}, [O_1, \cdots, O_n])$ where $\mathcal{A}$ is the plot evolution model. The objective of the refinement is to provide, for each plot, a sequence $[K_1, \cdots, K_n]$ where $K_1 \subseteq \mathcal{C}, \cdots, K_n \subseteq \mathcal{C}$ and where the "quality" of $[K_1, \cdots, K_n]$ is better than $[O_1, \cdots, O_n]$.
The criteria that enable us to judge the quality of K_i are:

- the cardinal of K_i: the fewer plausible classes in K_i, the better it is. The best case is when K_i is restricted to one class.
- "validity" correctness: the real landcover type should belong to K_i. If a ground truth is available for this plot, K_i and the class given by the ground truth are compared in order to assess the accuracy of the classification.

The refinement is realized in two steps. The evolution model of the plot $\mathcal{A}$ is used in simulation to determine the set of expected data at time t_i, denoted E_i with $E_i \subseteq \mathcal{C}$. A matching is applied between the observation and the expected data. The matching process is illustrated in Figure 1 and is defined as follows. Let O_i be the observation at t_i. Let $\otimes$ be the matching operator such that $K_i = O_i \otimes E_i$. In the following, since sets of classes are considered, the matching operator is the intersection. The matching may be extended to probabilistic or ranking data where the operator represents any fusion or combination rule. Expected data are provided by simulation according to a prediction or a postdiction mechanism.

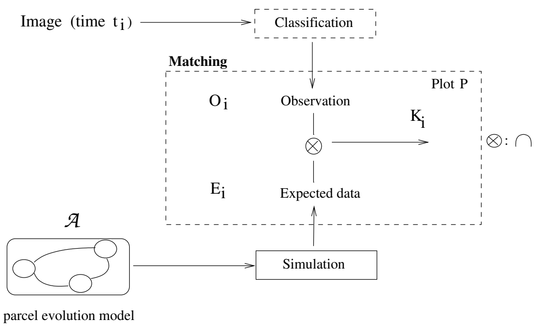

Figure 1. Refinement of the classification: simulation and matching

Prediction. We define the prediction mechanism as $< \mathcal{A}, K_{i-1}, t_i >$ where $\mathcal{A}$ is the model of the system, K_{i-1} is a state of the system at time t_{i-1} with $t_{i-1} < t_i$. Given the model and a state of the system at time t_{i-1}, the prediction mechanism consists in determining the state of the system for the current time t_i.

Postdiction. We define the postdiction mechanism as $< \mathcal{A}, K_{i+1}, t_i >$ where $\mathcal{A}$ is the model of the system, K_{i+1} is a state of the system at time t_{i+1} with $t_i < t_{i+1}$. Given the model and a state at time t_{i+1}, the postdiction mechanism consists in determining the state of the system for the current time t_i.

In order to refine the sequence of images, the method relies on both prediction and postdiction steps. We denote E'_i (resp. E_i) the set resulting from the prediction step (resp. postdiction step) and K'_i (resp. K_i) the set resulting from the matching in the prediction step (resp. postdiction step). K'_1 is the set of classes resulting from O_1, from which invalid classes at t_1 have been discarded, and is used to initialize the plot evolution model. The refinement algorithm, based on prediction and postdiction steps, is as follows.

Algorithm 1 Refinement of the plot classification

1- Prediction
Initialization:
$K'_1 \subseteq O_1$
for t_i, with $2 \leq i \leq n$ **do**
  Prediction: E'_i = prediction $< \mathcal{A}, K'_{i-1}, t_i >$
  Matching: $K'_i = O_i \otimes E'_i$
end for
2- Postdiction
Initialization: $K_n = K'_n$
for t_i, with $n-1 \geq i \geq 1$ **do**
  Postdiction: E_i = postdiction $< \mathcal{A}, K_{i+1}, t_i >$
  Matching: $K_i = K'_i \otimes E_i$
end for

In an ideal case, after the refinement of the classification there is no more confusion between classes and only one good landcover type is proposed in each K_i. Figure 2 shows the refinement of a classification on a sequence of 3 images.

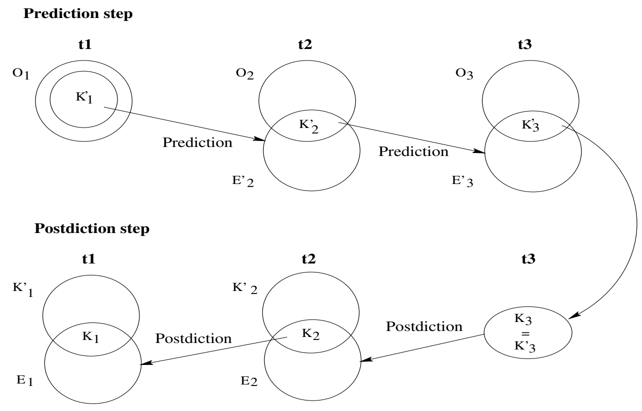

The sets of result classes for t,l t2, t3 are: K1, K2, K3
At time ti
Oi : observation resulting from the preliminary classification
E'i : set of classes resulting from the simulation in prediction
Ei : set of classes resulting from the simulation in postdiction
K'i : set of classes resulting from the matching in the prediction step
Ki : set of classes resulting from the matching in the postdiction step

Figure 2. Prediction and postdiction on 3 dates

4 Plot evolution modeling

This section gives an intuitive definition of timed automata and presents the plot evolution model represented using this formalism. A more formal description of the model can be found in [10].

4.1 Timed automata

The formalism of timed automata have been first proposed in [2] to model and analyze the behavior of real-timed systems. A timed automaton is a finite-state machine extended with a set of clocks which are real-valued variables that measure time. Clocks increase at a uniform rate and constraint the time at which transitions between states occur. Several independent clocks may be defined for the same timed automaton. They define timing constraints associated to *location*, the vertices of the graph, or transitions. In a timed automaton, time can elapse in a location as long as its timing constraint, called it's *invariant*, is true. Transitions are instantaneous and allow the reset of clocks. A formal definition a timed automata will be found in [2].

Example. Consider the timed automaton, shown in Figure 3, having two locations s_0 and s_1 and one clock x. This timed automaton models the behavior of a vending machine delivering tea or coffee. In location s_0 the system is waiting for the user to introduce coins into the machine. When the user puts coins, the system moves to the location s_1 and resets the clock. The machine is ready two seconds after the coins have been introduced and asks the user which has 10 seconds to make his choice: tea or coffee. The system can stay 12 seconds in the state s_1 which is modeled by the invariant condition $x \leq 12$. If the user makes his choice before the invariant has been violated (that is to say between 2 and 12) the machine gives him the drink and the system goes back to location s_0. If at time $x = 12$, no choice has been done, the system gives back the money before returning to location s_0.

The formalism of timed automata allow us to express uncertainty

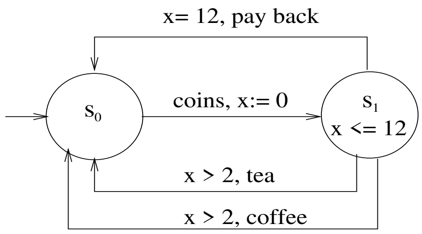

Figure 3. Timed automaton of a drinks machine

on timing constraint over transitions. Hence in the previous example, transitions labeled with tea or coffee can be triggered during the uncertain interval [2,12]. The main feature of the plot evolution system is its non-determinism, due to meteorological reasons or availability of machinery or labor. Therefore the system can be in multiple states at the same time which can be expressed with the uncertainty of timing constraints over transitions. Since a property of timed automata allows us to reset clocks on transition, we will be able to develop one generic model for several years of study.

4.2 The model

Timed automata appears to be the more convenient formalism to model plot evolution. We consider landcover classes, provided by the preliminary classification, as the locations of a timed automaton. Dates of crop calendars are expressed in a number of days between 0 and 365 and September 1 has been defined as the beginning of the crop cycle. In order to count days and years, we define two clocks: x, referring to the day, and y, referring to the year. Clocks x and y are initialized at September 1 of the first cycle of study. The clock x is reset each year thus the value of x corresponds to the value of y modulo 365 days.

The automaton is composed of several sub-automata each of which refers to the evolution of one crop (corn, wheat, rape plant, etc.) or to invariant landcover types (water, forest, etc.). Each sub-automaton follows the same topology: an initial location *init crop* which represents the entry in the crop (the clock x is reset on output edges), locations describing crop states, and a final location *end crop* from which begin all possible transitions towards successive crops.
Figure 4 illustrates a simple version of a plot evolution model using a timed automaton. The data set used for this study was acquired from interviews with agronomists about a watershed near Rennes (France). The evolution of crops, *wheat* and *corn*, and the landcover *water* are defined by this automaton. Doted lines express edges towards other sub-automata not represented here. Let us detail the corn evolution scenarios. At the beginning of the cycle, several locations are possible: *corn* (resulting from a previous cultivation not yet finished), *stubble* or *bare soil*. During the winter the soil can be bared or cultivated with *grassland* which is sown between September 10 (10) and November 15 (76). The *grassland* is cut between February 1 (153) and May 1 (243) whereas the *corn* could appear since April

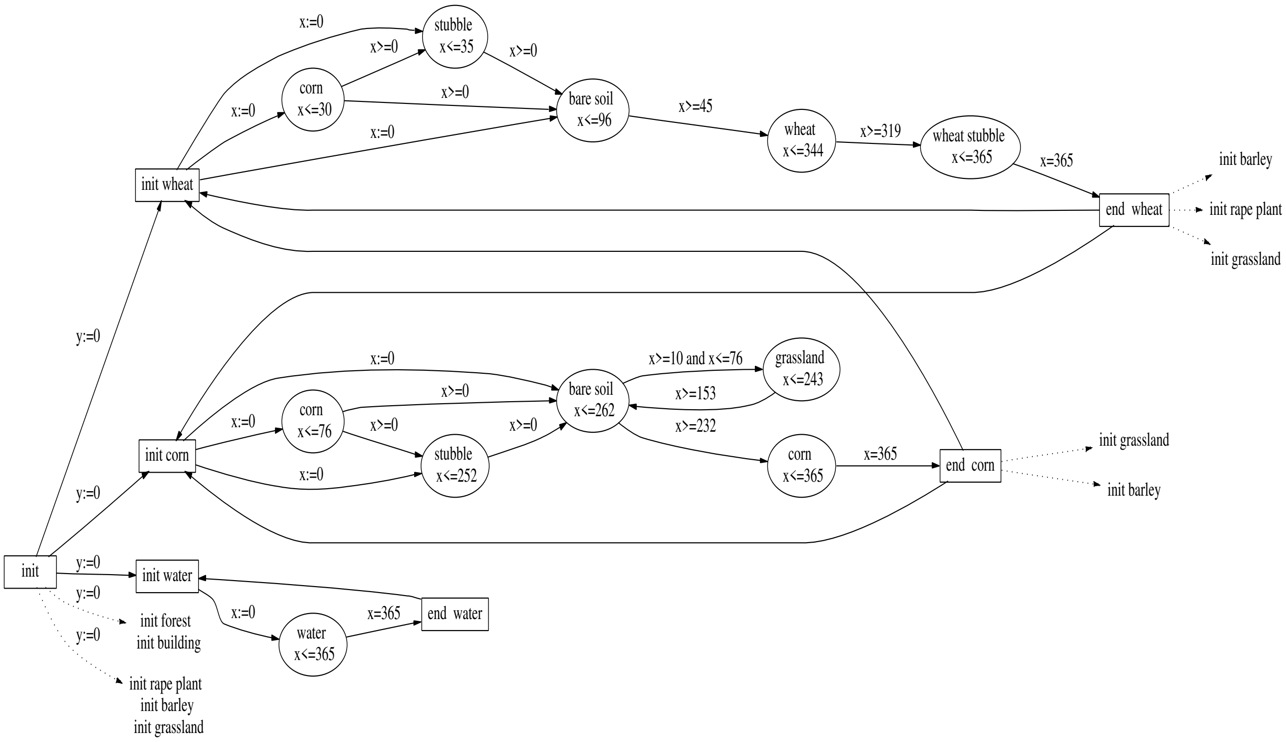

Figure 4. plot evolution model using a timed automaton

20 (232). Corn allows two kinds of crop harvest: early (from 0 to 30) or normal (from 30 to 60). Thus, states of corn has to be defined in cycles of successive possible crops. This is the case of wheat, which allows a corn harvested early (a *corn* state with the invariant $x \leq 30$), and of corn, which allows both harvest of a previous corn (a *corn* state with the invariant $x \leq 76$). The automaton we have developed contains 40 states and 62 transitions.

The refinement algorithm, introduced in Section 3 as Algorithm 1, has been precised in order to define the plot evolution model $\mathcal{A}$ with the timed automata formalism. This algorithm and the implementation, realized with the tool Kronos [16], are detailed in [10].

5 Experimental Results

The method has been applied on the five images of the sequence. To assess the accuracy of the classification, according to criteria presented in the problem definition, we have a dual objective. The first one is to increase the number of clear plots between the result of the preliminary classification and the result provided by the classification, and the second one is to obtain a reasonable identification rate, τ_i for each image.

During the refinement of the classification, each time a class is discarded from the set of plausible classes, its probability is equitably added on the others having a value greater than 0. Then, after the refinement, the class chosen to compute the identification rate is the one, none discarded by the method, having the maximum probability. Table 3 lists the results obtained after the refinement of the classification.

The result clearly shows the progression of the number of clear plots on all images (up to 54.3% for image I_3). Since the number of sample plots is low, the identification rate is only used to assess the coherence of the results. In this experiment, the identification rate remains reasonable for all images and even increases for the last three images of the series.

I_i	τ_i	clear plots		ambiguous plots	
I_1	90.91%	2030	95.6%	88	4.1%
I_2	86.90%	1908	89.8%	175	8.2%
I_3	81.08%	1948	91.8%	154	7.2%
I_4	69.16%	1813	85.4%	306	14.4%
I_5	75.70%	1594	75%	530	25%

Table 3. Refinement of the classification results

An example of an error matrix given for the image I_5 is shown in Table 4. The values provided by the preliminary classification and after the refinement are represented in normal and bold text respectively. For instance, in the matrix error, we can see that two samples known as wheat are better classified after the refinement since moving from corn and urban classes to wheat class. Three sample plots of grassland, firstly classified in the urban and wheat classes, belong

	wheat		grassland		corn		other		forest		water		urban		stubble	
wheat	8	**10**	1	**2**	2	**1**	0	**0**	0	**0**	0	**0**	0	**0**	0	**0**
grassland	6	**6**	28	**31**	11	**7**	0	**0**	5	**4**	0	**0**	2	**1**	2	**2**
corn	1	**0**	2	**2**	9	**15**	0	**0**	0	**0**	0	**0**	0	**0**	0	**0**
other	0	**0**	0	**0**	0	**0**	2	**2**	0	**0**	0	**0**	0	**0**	0	**0**
forest	0	**0**	2	**0**	0	**0**	0	**0**	6	**7**	0	**0**	0	**0**	0	**0**
water	0	**0**	0	**0**	0	**0**	0	**0**	0	**0**	5	**5**	0	**0**	0	**0**
urban	1	**0**	2	**0**	1	**0**	0	**0**	0	**0**	0	**0**	5	**6**	0	**0**
stubble	0	**0**	1	**1**	0	**0**	0	**0**	0	**0**	0	**0**	0	**0**	5	**5**
total	16		36		23		2		11		5		7		7	

Table 4. Error Matrix of Image 5

	I_1	I_2	I_3	I_4	I_5
ground truth	-	-	-	wheat	wheat
observation OBS_i	wheat (1)	wheat (1)	wheat(0.84) grassland(0.16)	grassland(0.40) wheat(0.36) corn(0.24)	grassland (0.70) corn (0.14) forest (0.16)
prediction E'_i	$\rightarrow$ -	$\rightarrow$ wheat stubble	$\rightarrow$ wheat grassland	$\rightarrow$ wheat grassland corn	$\rightarrow$ wheat grassland corn
matching K'_i	wheat	wheat	wheat grassland	wheat grassland corn	grassland corn
postdiction E_i	$\leftarrow$ -	$\leftarrow$ wheat stubble grassland	$\leftarrow$ grassland	$\leftarrow$ grassland corn	$\leftarrow$ grassland corn
matching K_i	wheat	wheat	grassland	grassland corn	grassland corn
choice	**wheat**	**wheat**	**grassland**	**grassland**	**grassland**

Table 5. Misclassification of a plot due to preliminary classification error

after the refinement to the grassland class. The corn class have gained six samples previously put in the grassland class (4), in the wheat class (1) and in the stubble class (1). One sample of forest, previously known as grassland, has rejoined its class.

The misclassification remaining after the refinement is due to three types of problems: 1) the good class is not given by the preliminary classification in the probability distribution, 2) the plot is still ambiguous after the refinement and the maximum of probability does not propose the good class, 3) the initialization of the model is not reliable enought to have good prediction. In order to explain why some samples remain misclassified whereas their landcover types are consistent with the plot evolution model, Table 5 presents the reasoning and the result for a particular plot. This is the case of the plot #635 which is known to be a plot of wheat but is classified as grassland even after the refinement.

This example shows misclassification due to an error of the preliminary classification. Since this classification does not propose the wheat in the set of possible classes for the image I_5, the method can not give it at as a result and provides another sequence of classes, however consistent with the plot evolution model, but none with the ground truth.

For the moment, the method does not deal with the non labeled plots, obtained when the intersection between the observation and the set of expected data is null (that is to say when $O_i \cap E'_i = \emptyset$). The number of plots concerned with this situation are for the image successions $I_1 \rightarrow I_2$: 985, $I_2 \rightarrow I_3$: 366, $I_3 \rightarrow I_4$: 503 and $I_4 \rightarrow I_5$: 389. When this situation happens, the method affects to the plot the subset $K_i \subseteq O_i$ of possible classes at t_i.

We have conducted another experiment where the number of images and the first image of the sequence have varied. The analysis of the evolution of clear plots is illustrated in Table 6. It shows the respective contributions of prediction and postdiction.

	I_1	I_2	I_3	I_4	I_5
I_1	-	**242**	**0**	**0**	**0**
I_2	209	-	**2**	**0**	**0**
I_3	0	174	-	**806**	**172**
I_4	0	39	244	-	**572**
I_5	0	28	93	932	-

Table 6. Contribution of prediction and postdiction

Lines represent the number of new clear plots resulting from the refinement for the images I_1 to I_5 and columns $I_1 - I_5$ represent the contribution of the images during the prediction and postdiction steps (shown in ordinary and bold type, resp.). If we take image I_3, image I_2 contributes 174 clear plots in the prediction step, and images I_4 and I_5 contribute 806 and 172 clear plots respectively in the postdiction step.

6 Conclusion

In this article we have proposed a new classification approach based on the plot evolution model using a timed automata formalism. Our objective was to deal with both a temporal model and a timed sequence of images, in order to refine a preliminary classification. The application of the method used to provide a thematic map at each date given a sequence of 5 images, has demonstrated successful results. The main advantages of the proposed method are to be stressed:

- A preliminary classification avoid us dealing with low-level process on images. In this application a supervised classification has been applied because of the simplicity of the classifier but an unsupervised method should be employed similarly.
- The *a priori* knowledge used by the model is restricted to agricultural knowledge easy to collect from expert of the area. This knowledge is sensor independent and allow us to use any kind of images. The uncertainty about the dates resulting from the environment is taking into account by the model and the simulation process.
- The results provided by the classification are globally better since the number of clear plot increases on all the images and the identification rate is consistent.

We plan to apply this method on another sequence of images representing the Vittel site (located in the north-east of France). Finally, actual studies are conducted in order to integrate probabilities of data resulting from the preliminary classification and of data given by the simulation of the plot model. A new matching operator, dealing with probabilities, has to be defined as well as a new decision rule used to choose a preferred class when ambiguous plots remain at the end of the refinement process.

REFERENCES

[1] J. Adinarayana and N. Rama Krishna, 'Integration of multi-seasonal remotely-sensed images for improved landuse classification of a hilly watershed using geographical information systems', *International Journal of Remote Sensing*, **17**(9), 1679–1688, (1996).

[2] R. Alur and D.L. Dill, 'A theory of timed automata', *Theoretical Computer Science*, **126**(183), 235, (1994).

[3] Arkemie. http://ourworld.compuserve.com/homepages/arkemie/, 1996.

[4] V. Clément, G. Giraudon, S. Houzelle, and F. Sandakly, 'Interpretation of Remotely Sensed Images in a Context of Multisensor Fusion Using a Multispecialist Architecture', *IEEE Transaction on Geosciences and Remote Sensing*, **31**(4), 779–791, (July 1993).

[5] C. Corves and C.J. Place, 'Mapping the reliability of satellite-derived landcover maps : an example from the central amazon basin', *International Journal of Remote Sensing*, **15**, 1283–1294, (1994).

[6] J. Desachy, L. Roux, and E.H. Zahzah, 'Numeric and symbolic data fusion: A soft computing approach to remote sensing images analysis', *Pattern Recognition Letters*, **17**, 1361–1378, (1996).

[7] D.G. Goodenough, M. Goldberg, G. Plunkett, and J. Zelek, 'An Expert System for Remote Sensing', *IEEE Transactions on Geoscience and Remote Sensing*, **GE-25**(3), 349–359, (May 1987).

[8] K. Johnsson, 'Segment-Based Land-Use Classification', *Photogrammetric Engineering & Remote-Sensing*, **60**(1), 47–53, (January 1994).

[9] B. Kartikeyan, K.L. Majumder, and A.R. Dasgupta, 'An Expert System for Land Cover Classification', *IEEE Transactions on Geoscience and Remote Sensing*, **33**(1), 58–66, (January 1995).

[10] C. Largouët and M-O. Cordier, 'Timed Automata Model to Improve the Classification of a Sequence of Images', in *European Conference of Artificial Intelligence (ECAI)*, (2000).

[11] F. Le Ber, 'Un système multi-agents d'aide à l'interprétation d'images satellitaires', *9 ème Congrès Reconnaisance des Formes et Intelligence Artificielle*, 507–518, (1994).

[12] T. Matsuyama, 'Knowledge-based Aerial Image Understanding Systems and Expert Systems for Image Processing', *IEEE Transaction Geoscience of Remote Sensing*, **GE-25**, 305–316, (1987).

[13] D. M. McKeown, W.A. Harvey, and J. McDermott, 'Ruled-based interpretation of aerial imagery', *IEEE Transactions on Pattern Analysis and Machine Intelligence*, **7**(5), 570–585, (1985).

[14] H. Shimoda, S.Hong, K. Fukue, and T. Sakata, 'A Multi-temporal Classification Method using Dempster-Shafer Model', in *International Geoscience and Remote Sensing symposium IGARSS11*, Espoo Finland, (1991).

[15] J.K. Wu, D.S. Cheng, and W.T. Wang, 'Model based remotely-sensed imagery interpretation', *International Journal of remote-sensing*, **9**(8), 1347–1356, (1988).

[16] S. Yovine, 'Kronos : A verification tool for real-time systems', *International Journal of Software Tools for Technology Transfer*, **1**, (1997).